A Novel Route to Inducing Disorder in Model Polymer-Layered Silicate Nanocomposites

Mary Kurian,[†,§] Arnab Dasgupta,[⊥,†] Mary E. Galvin,[*,†,§] Christopher R. Ziegler,[‡] and Frederick L. Beyer[*,‡]

Department of Materials Science & Engineering, University of Delaware, Newark, Delaware 19716, and Materials Division, U.S. Army Research Laboratory, Aberdeen Proving Ground, Maryland 21005

Received November 18, 2005; Revised Manuscript Received December 29, 2005

ABSTRACT: The effects of the degree of silicate surface modification by organic surfactants and the nature of surfactant−matrix enthalpic interactions on polymer-layered silicate nanocomposite (PLSN) morphology have been systematically investigated. Using cation exchange to modify montmorillonite, a series of "partially" modified clays were prepared and used in turn to fabricate polystyrene (PS)−, poly(vinyl methyl ether) (PVME)−, and poly(methyl methacrylate) (PMMA)−matrix PLSNs via static melt intercalation. Small-angle X-ray scattering and transmission electron microscopy revealed that the morphological behavior of the PS-based "partial" coverage PLSNs was seemingly dependent on surfactant length, with the shortest surfactant providing the most significant disruption of the clay tactoids. Examination of the PMMA- and PVME-based PLSNs indicated that the nanocomposite morphology was only weakly affected by the nature of matrix−surfactant enthalpic interactions. The results of modifying montmorillonite with 5.5 kg/mol PS-based surfactant at only 4.7% coverage and subsequent fabrication of PLSNs via static melt intercalation confirmed that clay tactoids can be disordered through appropriate control of the degree of surfactant coverage for a given surfactant length.

Introduction

Polymer-layered silicate nanocomposite (PLSN) materials have been extensively researched beginning with the work from the Toyota research laboratories showing that the incorporation of a few weight percent of a layered silicate clay mineral such as sodium montmorillonite in a suitable polyamide polymer matrix resulted in composites with significantly enhanced physical properties.[1] Since that time, a large body of work has been amassed which reports advances in both fabrication techniques and the wide variety of matrix polymers employed to create PLSNs.[2−19] Despite their great promise, PLSNs have not achieved the anticipated use in a broad range of applications. This is due primarily to the inability to control dispersion of the individual clay layers, limiting the properties of the final nanocomposite.

The incorporation of a naturally occurring, layered hydrophilic mineral into an organic polymer matrix that is often hydrophobic is a nontrivial task. Typically, the best dispersion of clay layers is achieved when either solution processing methods or in situ polymerization of monomer are viable routes to the final material. For most polymers, however, these routes are not feasible, and compatibilization of the clay is required. Many groups have reported on the different types of modification schemes used to prepare organophilic clays for incorporation into polymer matrices.[20−33] In most of these examples, commercially available quaternary alkylammonium compounds were used to modify the clays before their incorporation into a polymer matrix.

The most common mechanical mixing technique used in nanocomposite fabrication is melt processing using twin screw extrusion. Extrusion processing in this manner applies tremendous shearing forces to the melt, breaking up the micron-sized clay tactoids and dispersing the clay layers in the melt. Several aspects of this process are noteworthy. First, this process is energy intensive, requiring a substantial amount of energy to fully disperse the clay. Second, as a result of the extreme forces required to disrupt the clay tactoids, both the clay layers and the polymer matrix can be degraded by this process. Finally, it has been noted that further processing of the PLSN can actually result in reflocculation of the clay layers into a more closely associated group similar to an intercalated clay tactoid, robbing the final PLSN of the benefits of full clay dispersion. Jang et al.[34] have noted that in-situ polymerization produces materials that, after a subsequent melt-processing step, can revert back to an intercalated morphology. Similar reorganization behavior of the nanocomposite structure has been reported by Manias et al.[35] in their studies on the stability of nanocomposite "hybrids" that after precipitation from solution were subjected to further processing at an elevated temperature, via compression molding or mixing in a twin-screw extruder. A significant advantage would be gained from the ability to control nanocomposite morphology and form materials that are at thermodynamic equilibrium without compromising the integrity of the mineral or matrix materials.

In both this study and previous efforts, the research goal has been to develop a PLSN system that, at equilibrium, would exfoliate primarily because of thermodynamic interactions between the three components of the PLSN: phyllosilicate clay mineral, organic modifier, and matrix polymer. Such a system would have several distinct advantages, most notably requiring minimal processing for the dispersion of the clay filler. The theoretical framework developed by Balazs and co-workers[36,37] provides a useful starting point for the design of suitable experimental systems, aiding a systematic investigation of the parameters that control and influence PLSN morphology. A parameter defined in the theoretical model that captures the

* Corresponding authors. E-mail: galvinme@airproducts.com; flbeyer@arl.army.mil.
† University of Delaware.
‡ U.S. Army Research Laboratory.
§ Current address: Air Products & Chemicals, Inc., 7201 Hamilton Blvd., Allentown, PA 18195.
⊥ Current address: Indium Corporation of America, 34 Robinson Road, Clinton, NY 13323.

10.1021/ma052478z CCC: $33.50
Published on Web 02/01/2006

nature and influence of enthalpic interactions in the system is the polymer−surfactant interaction parameter, χ. Here, χ is equivalent to a Flory−Huggins binary segmental interaction parameter. A negative value of χ indicates miscibility, and a positive value indicates immiscibility. It has been postulated that even weakly favorable interactions between these components will result in the formation of an exfoliated morphology in the final nanocomposite material, similar to the ease with which hydrophilic poly(ethylene oxide) (PEO) is intercalated into clay galleries.[38,39] Additionally, the length of the surfactant used to modify the silicate has been predicted to significantly influence the morphology of the resultant nanocomposite material. Those arguments suggest that longer surfactants would be more useful in promoting intercalation and exfoliation since they could provide a greater reduction in entropic penalty to the polymer molecules intercalating the confined gallery spaces.

In two previous studies, two different series of organically modified clays were prepared by treating montmorillonite with PS-based surfactants.[40,41] The molecular weight of the surfactants varied from 2 to 18 kg/mol. In the first,[40] the clay was modified to the fullest extent possible, based on the cation exchange capacity of the clay mineral. These "full coverage" modified clays were incorporated into a PS matrix, having a molecular weight of ∼10 kg/mol, by direct melt intercalation.[42] No shear was applied during direct melt intercalation, meaning that any change in morphology was a result of thermodynamic driving forces. Irrespective of surfactant molecular weight, only phase-separated morphologies were observed for these materials, a result explained by well-accepted theories of autophobic dewetting from dense polymer brushes.[43] To counter these effects, a second series of organoclays were prepared, also having complete coverage of the available sites for cation exchange, but using binary mixtures of surfactants of different chain lengths ("mixed coverage").[41] Though the intended "roughening" of the silicate surface using this strategy resulted in increased local disorder, potentially beneficial for intercalation and exfoliation, this effect also did not result in intercalation of the polymer matrix into the clay galleries.

In the current study, the morphological behavior of PLSNs with only partial surfactant modification of the clay has been examined. Two different degrees of cation exchange, "partial" and "very low", have been considered. The target level of partial cation exchange by the PS-based surfactants was based on specific values used in the Balazs model and found for these materials to be ca. 17% of the available cation exchange sites in the specific clay used here. The target surfactant areal density of the samples exchanged to very low coverage was dependent on the molecular weight of the associated surfactant. These values were determined empirically on the basis of preliminary experimental results. Furthermore, the effect on PLSN morphology of the enthalpic interactions (as given by χ) between the PS-based surfactant modifier and the polymer matrix has been examined using alternative polymer matrices such as poly(vinyl methyl ether) (PVME) and poly(methyl methacrylate) (PMMA). As with previous experiments using these PS-based surfactants, the intent of these experiments was to determine whether nanocomposite morphology can indeed be controlled by the suitable modification of the inorganic layered silicate used in its fabrication, without the use of intensive processing schemes.

Experimental Section

"Wyoming bentonite" montmorillonite-layered silicate clay mineral "SWy-2" (Na-MMT) was purchased from the Source Clay Minerals Repository at the University of Missouri (now available through Purdue University). To rid the clay of impurities, ∼10 g of clay were dispersed in 1 L of deionized water, and the suspension was allowed to stand for several hours to achieve sedimentation of the heavier impurity fractions. The supernatant was decanted and centrifuged to further remove impurities and recover the cleaned clay. This material was vacuum-dried to remove water and then ground using a mortar and pestle. The cation-exchange capacity (CEC) was determined by standard soil analysis techniques[44,45] to be approximately 67 mequiv/100 g dry clay, which was in reasonable agreement with the supplier's quoted value of 76 mequiv/100 g. This measured value of CEC and a total surface area of 800 m^2/g[46] were used in all calculations of the degree of coverage of the silicate surface by the surfactant.

Table 1. MALDI Mass Spectrometric Data for Molecular Weights of Quaternary Ammonium Ion End-Terminated PS-Based Surfactants

surfactant	M_w (g/mol)	M_n (g/mol)	PDI
Q-2	1820	1735	1.05
Q-3	2800	2700	1.04
Q-5	5688	5561	1.02
Q-7	7000	6800	1.03

Matrix polymer materials used were purchased from Polymer Source (Dorval, Quebec, Canada). Low-polydispersity PS (P3005-S, $M_n \sim 11$ kg/mol, PDI ∼ 1.05), PVME (P2209-MVE, $M_n \sim 11.5$ kg/mol, PDI ∼ 1.06), and PMMA (P4078-MMA, $M_n \sim 11.5$ kg/mol, PDI ∼ 1.08) were used as received. Low-polydispersity quaternary ammonium end-functionalized PS surfactants of four different molecular weights were synthesized and fully characterized as reported previously.[40] Table 1 lists the properties of these surfactants, showing the effectiveness of the synthetic scheme in preparing materials with well-controlled molecular weights. The nomenclature used describes the approximate molecular weight of the surfactant. For example, Q-2 refers to a quaternary ammonium end-functionalized PS surfactant of approximate molecular weight 2 kg/mol.

Modified clays having the required degree of surfactant coverage were prepared by a simple solution-based cation-exchange procedure. In the series termed "partial" coverage, a measured amount of Na-MMT clay was treated with the amount of surfactant of a given molecular weight calculated to yield a surfactant coverage of ∼17% of the total cation-exchange capacity of the clay. Individual solutions of the clay and surfactant, each in a 3:1 (v/v) mixture of acetone:water, were made and stirred for ∼8 h. The surfactant solution was then added to the clay dispersion with rapid stirring to maximize contact between the two components, and in most cases, the formation of a white precipitate was seen almost instantaneously. The mixed solution was allowed to stir for an additional 8 h, after which the precipitate was isolated by centrifugation and dried in vacuo at 60 °C for 12 h. Four different partially modified clays were prepared by this technique, one for each of the four surfactants used in this work.

To confirm that the actual compositions of the modified clays were in agreement with the calculated target compositions, thermogravimetric analysis (TGA) was performed for each of the modified clays. A Perkin-Elmer TGA 7 (Wellesley, MA) instrument was used to monitor the weight loss for 10 mg samples as they were heated from 30 to 900 °C at a rate of 10 °C/min. The residue at the end of the scan was taken as a measure of the total inorganic content in the sample. Efforts to directly measure the uniformity of the surfactant modification were not successful, but no evidence of unmodified clay was found by wide-angle X-ray diffraction, indicating that all the modified clay obtained by this procedure was fairly uniformly modified.

Nanocomposites using the modified clays were made by direct melt intercalation, an equilibrium melt intercalation process that has been described previously.[40] In this fabrication process, based on the TGA data for the modified clay, calculated amounts of modified clay and matrix polymer material were mixed such that the final PLSN contained 5 wt % inorganic matter with the remaining 95 wt % consisting of surfactant and the polymer matrix. This mixture was pressed into a pellet under minimal contact pressure and then annealed in vacuo for 1 week at a temperature

above the glass transition temperature, T_g, of the matrix polymer (PS-based PLSNs at 150 °C, PVME-based PLSNs at 60 °C, and PMMA-based PLSN at 150 °C). In previous studies, the length of time of annealing (1 week, 150 °C) for the PS-based materials was calculated to be well in excess of the length of time required for the diffusion of matrix homopolymer molecules into the center of a large clay tactoid.[40] The same PS matrix material, which has a molecular weight below the entanglement molecular weight of PS, and identical annealing conditions were used in the current work for the PS-based nanocomposites. The annealing process was necessarily different for the PVME-based materials because of the LCST miscibility behavior. An annealing temperature of 60 °C, while low relative to that used for the PS-based PLSNs, was necessary to remain well below the binodal phase separation boundary for the PS and PVME system.[47] The annealing temperature is sufficiently higher than the glass transition temperature (−28 °C) of the PVME matrix such that the 1 week annealing time was thought to be sufficient to allow the formation of the equilibrium morphology. To confirm that the PVME-based materials were exhibiting morphological behaviors indicative of a stable thermodynamic state and that the system was not kinetically limited, a second set of PVME nanocomposites was fabricated as above and annealed for 4 weeks at 60 °C. At the end of the annealing cycle, samples were cooled to room temperature in vacuo.

Small-angle X-ray scattering (SAXS) was used to characterize changes in the gallery height of the clay and monitor the morphology formation in the PLSNs. A Rigaku Ultrax18 (Rigaku MSC, Inc., The Woodlands, TX) rotating anode generator operated at 2.4 kW power was used as the X-ray source. A pyrolytic graphite crystal was used to monochromate the Cu Kα radiation, giving a wavelength, λ, of $\lambda = 1.5418$ Å. The sample-to-detector distance of 62.3 cm was calibrated using a silver behenate standard. The 2-dimensional scattering data were collected with a Molecular Metrology (Osmic, Inc., Auburn Hills, MI) multiwire area detector. Azimuthally averaged SAXS data are presented in terms of intensity, I, as a function of q, the magnitude of the scattering vector, which is given by $q = (4\pi/\lambda)\sin(\theta)$, where the scattering angle is 2θ and λ is the wavelength of the radiation. The length scale, d, corresponding to a given value of q is given by $d = 2\pi/q$, and the associated gallery height, h, is given by $h = (d - 10)$ Å. The primary Bragg reflections in the SAXS data were analyzed for peak position and breadth using Wavemetrics Igor Pro v. 5.04 (Portland, OR) and the "Irena" small-angle scattering data analysis procedures developed by Dr. Jan Ilavsky of Argonne National Laboratory. For strong reflections, the combination of a simple linear background and a Gaussian distribution was fitted to the data. For weak reflections, the linear background was not sufficient, and a power-law background was used instead. The coefficients for the power-law fit were fixed prior to optimizing the Gaussian distribution.

A JEOL 200CX TEM (Peabody, MA) operated at an accelerating voltage of 200 kV was used to image microtomed sections. Samples ~50 nm thick were ultramicrotomed for TEM using a Leica Microsystems FCS Ultracut microtome (Bannockburn, IL) and a Microstar diamond knife (Huntsville, TX). Sections were collected dry using a hair curl to prevent the morphology of the specimen from being altered by solvents often used for specimen collection.

Results and Discussion

For ease of data viewing, a standard nomenclature system has been utilized, where the sample composition is described by the sample name. For example, sample M-2P corresponds to a surfactant-modified clay, where "M" indicates montmorillonite clay, "2" indicates modification with surfactant Q-2 (having molecular weight of ~2 kg/mol), to a level of "partial" ("P") surfactant areal density (coverage). The corresponding PS and PVME matrix-based nanocomposites would be named M-2P-PS and M-2P-PVME, respectively. Table 2 lists the compositional details for the partially modified clays that were fabricated and characterized via TGA. Based on TGA results, the degree of coverage of the clay by the surfactant was calculated for each modified clay. The coverages were slightly higher than the 17% goal but are very similar. Nanocomposites made using each of the modified clays were also studied by TGA, and in all cases, the inorganic content was confirmed to be 5% of total sample weight.

Table 2. Composition and Surfactant Coverage Data for "Partially" Modified Clays Calculated from TGA Results

		composition (%)		
sample	surfactant	clay	organic	coverage (%)
M-2P	Q-2	82	18	19
M-3P	Q-3	72	28	22
M-5P	Q-5	60	40	18
M-7P	Q-7	52	48	20

Figure 1 shows the SAXS data collected for the "partial" coverage, PS-matrix-based samples. The data are presented in pairs, with the lower data set in each pair from the "partially" modified clay (without homopolymer) and the upper data set from the corresponding PLSN, as labeled beside each profile in the plot. The data are plotted on a log−linear scale and shifted vertically for clarity. A table is inset in the graph giving the scattering vector, q, and the corresponding gallery height, h, associated with the primary Bragg reflection for each sample.

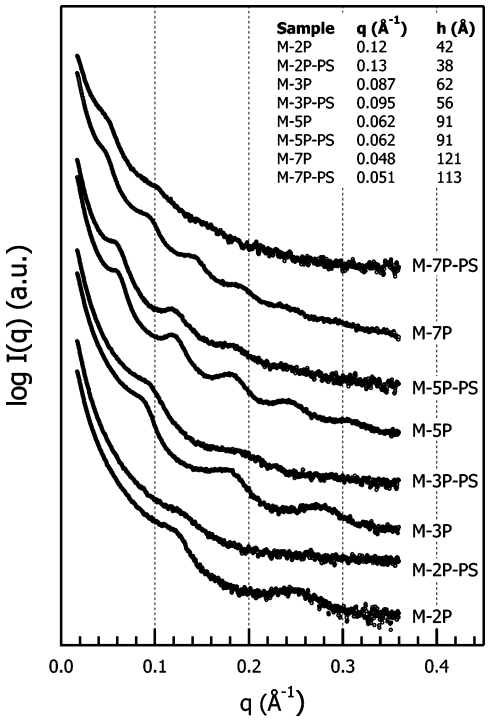

Figure 1. SAXS data for PS matrix-based nanocomposite materials incorporating PS-surfactant modified clays with "partial" coverage. The inset gives the corresponding position of the scattering maxima and gallery heights for the PS-based PLSNs.

Inspection of Figure 1 reveals several interesting trends. First, all the modified clays produce several orders of Bragg reflections, indicating that they are generally well-ordered, as is typical for these materials. The observed Bragg reflections are generally unchanged between the modified clay and the PLSNs for both M-3P-PS and M-5P-PS, indicating that little significant morphological change occurs with annealing. For M-7P-PS, the number and sharpness of Bragg reflections decrease somewhat, indicating a slight reduction of long-range order, even though the length of the Q-7 surfactant is closest to that predicted to induce exfoliation in the current experimental system, in the models developed by Balazs and co-workers. The most surpris-

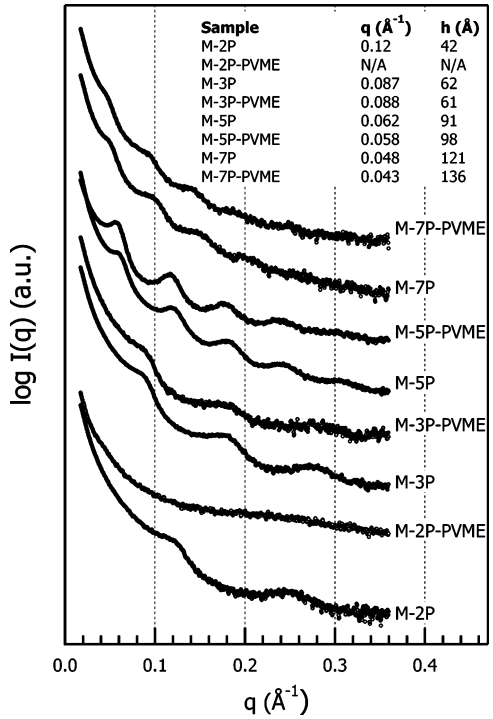

Figure 2. SAXS data for PVME matrix-based nanocomposite materials incorporating PS-surfactant-modified clays with "partial" coverage. The inset gives the corresponding position of the scattering maxima and gallery heights for the PVME-based PLSNs.

ing data, however, are for the samples M-2P and M-2P-PS, based on the shortest surfactant, Q-2. There are fewer reflections in the M-2P modified silicate as compared to the silicates modified with longer surfactants (M-3P, M-5P, and M-7P), indicating that there is inherently some disruption of order between silicate sheets in the surfactant-modified M-2P clay even by itself. After annealing, the Bragg reflections from the M-2P−PS nanocomposite almost completely vanish, indicating that the ordered stacks of clay layers that give rise to these diffraction peaks have been completely disordered in some way. It is important to note that the absence of Bragg reflections in the SAXS data cannot, by itself, be taken as proof of an exfoliated PLSN morphology. While this assertion is often made and reported in the literature, the inability to unambiguously extract from X-ray scattering data the real-space scattering length density distribution function requires that any morphological assertion be supported by a combination of a bulk characterization technique, such as X-ray scattering, and complementary real-space information obtained by microscopy. An absence of Bragg diffraction peaks means only that there are no areas of the sample in which the scattering length density fluctuations are periodic.[48] Specifically, disordering of the second kind noted by Vaia and Liu could lead to a morphology that would produce no Bragg reflections but also not be exfoliated.[49]

Samples based on a PVME matrix were specifically fabricated to investigate the effect of favorable enthalpic interactions ($\chi < 0$) between the surfactant and the matrix on the final nanocomposite morphology. Depending on the relative strengths of the entropic and enthalpic forces within the PLSN system, favorable enthalpic interactions might be expected to produce intercalation of PVME homopolymer into the PS-modified clay galleries. The value of the Flory−Huggins χ parameter for the [PS−PVME] pair at room temperature is −0.0412. The [PS−PVME] χ parameter remains negative throughout the annealing process, increasing to −0.0261 at 60 °C.[47] The SAXS data presented in Figure 2 generally indicate that the morphological behaviors of the PS-based and PVME-based materials are nearly identical; in Figure 2 the essential behaviors noted for Figure 1 are repeated.

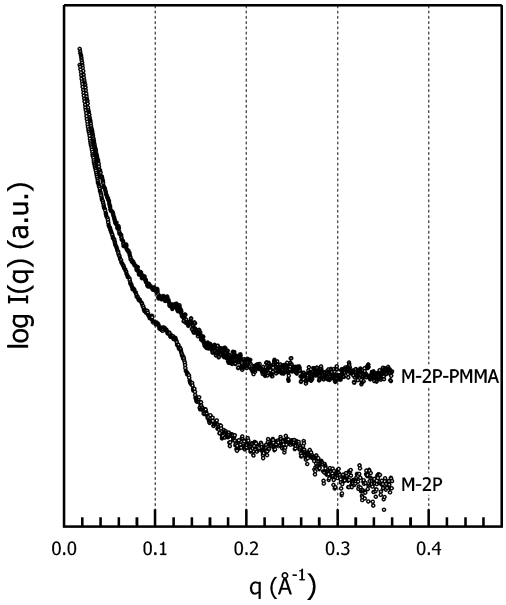

Figure 3. SAXS data for a PMMA-based PLSN based on M-2P.

The data for the modified clays alone are identical to those shown in Figure 2 as the same stock samples were used. Samples M-3P-PVME and M-5P-PVME both show qualitatively the same SAXS patterns and the same gallery heights as the corresponding modified clays, indicating that no intercalation occurred in these materials. A slight decrease in the clarity of the Bragg reflections along with a slight increase in gallery height is seen for M-7P-PVME, as was found for M-7P-PS. Most notably, the same dramatic loss of Bragg diffraction peaks is observed for sample M-2P-PVME that was seen for M-2P-PS. While the SAXS data for M-2P-PS do show a faint Bragg reflection, no reflection was measured for M-2P-PVME. Further annealing the PVME-based PLSNs for an additional 3 weeks resulted in no changes observable via SAXS, indicating that the PVME-based materials were thermodynamically stable and that the system is not kinetically limited. Consequently, the observed morphology is unlikely to change on any reasonable experimental time scale. Thus, at this low level of miscibility, favorable enthalpic interactions appear to make only a small contribution to morphological behavior. Intercalation does not occur, except possibly for M-2P-PS and M-2P-PVME.

Although not predicted to enhance intercalation or exfoliation, a PLSN was fabricated using the modified clay M-2P in conjunction with PMMA as the matrix material. Immiscible PS and PMMA have a Flory−Huggins χ parameter of 0.0195 at room temperature.[47] The same direct melt intercalation technique, at an annealing temperature of 150 °C, was used to fabricate the PLSN, M-2P-PMMA. At the annealing temperature, χ is reduced only slightly to 0.0175. Figure 3 shows the SAXS data collected for the M-2P-PMMA sample in comparison to that of the modified clay.

Surprisingly, the PLSN again shows a marked decrease in the intensity of Bragg reflections, in this case showing only a weak and broad primary Bragg reflection. These data perhaps most firmly enforce the small role that enthalpic interactions between surfactant and matrix polymer play in determining morphological behavior.

The most striking result obtained was the disordering of the clay tactoids in the M-2P-based samples, both the modified clay

Table 3. Calculated Values for "Required" and "Available" Areas per Cation on the Silicate Surface (in Å^2), for the PS-Based Surfactants of Varying Molecular Weights, at Different Extents of Silicate Modification by the Surfactants

surfactant	MW (g/mol)	R_g (Å)	area/cation required (based on R_g)	area/cation available (at 100% coverage)	area/cation available (at 17% coverage)	area/cation available (at 4.7% coverage)
Q-2	1735	11	380	178	1047	3825
Q-3	2700	14	616	*a*	*a*	*a*
Q-5	5561	21	1386	*a*	*a*	*a*
Q-7	6800	23	1662	*a*	*a*	*a*
Q11	11200	29	2643	*a*	*a*	*a*
Q18	17600	37	4302	*a*	*a*	*a*

[a] Available areas are fixed and independent of the surfactant characteristics and depend only on the silicate surface area, its cation exchange capacity and the level of modification/coverage by surfactant.

and the three corresponding nanocomposites, particularly given that it was predicted from both the Balazs model and established brush theory that longer surfactants would be most likely to allow intercalation to occur by best reducing the entropy penalty incurred by a polymer confined to a clay gallery. In previous studies where nanocomposites were made using clay that was completely exchanged, modified by either a single surfactant (full coverage) or a mixture of surfactants (mixed coverage), no change in morphology was ever observed for PLSNs fabricated via direct melt intercalation. On the basis of those results, the current samples were fabricated so that the clay was only partially modified in order to provide enough modifier to compatibilize the silicate with the polymer matrix while avoiding the formation of dense brushes that were previously seen. Even at the reduced level of surfactant modification, longer surfactants continue to show evidence of phase separation, even when $\chi < 0$. However, the general absence of Bragg reflections in the SAXS data for M-2P-PS and M-2P-PVME and the marked reduction in diffraction from M-2P-PMMA indicate the near-total disruption of the clay tactoids in some fashion. These results seem to indicate that at the level of partial coverage nanocomposite morphology may be dependent on the length of the surfactant used to modify the clay, with very short surfactants being beneficial to tactoid disordering.

It is also possible, however, that the surfactant areal density rather than the surfactant length might be the driving factor that controls nanocomposite morphology. It can be envisioned that at a given level of coverage surfactants having different lengths would differ in their spatial distributions and conformations within the interlayer spaces and thus strongly influence the final nanocomposite morphology. A rough estimate of the silicate surface area, A, required by an unperturbed surfactant cation can be calculated as $A = \pi R_g^2$, where R_g is the radius of gyration for a given surfactant. In this calculation, interactions with the silicate surface, likely to be repulsive, are neglected. At the coverage where the area available to a surfactant chain equals πR_g^2, the chain can take on a conformation equivalent to that found in a bulk sample, i.e., an equilibrium conformation. If the area required for the cation to adopt an equilibrium conformation is higher than the actual area available to the cation (such as in high surface coverage conditions), then the surfactant chains must adopt an extended chain conformation and in the extreme case form a dense brush on the silicate surface, as seen in our previous studies.[40,41] If, however, the area required for the surfactant chain to adopt an equilibrium conformation is less than the area available to the cation (low surface coverage), then the coverage of chains on the silicate surface is such that neighboring surfactants do not interact; in the terms of Leibler's brush theory, this would be the mushroom regime.[43]

Table 3 summarizes the calculations of required and actual silicate surface areas for the series of surfactants used in this report, at the different coverages studied in both the current and the previous reports. It should be noted that the area available per cation at a given degree of surfactant coverage is independent of surfactant length and dependent only on the surface area of the clay, the cation-exchange capacity, and that particular coverage.

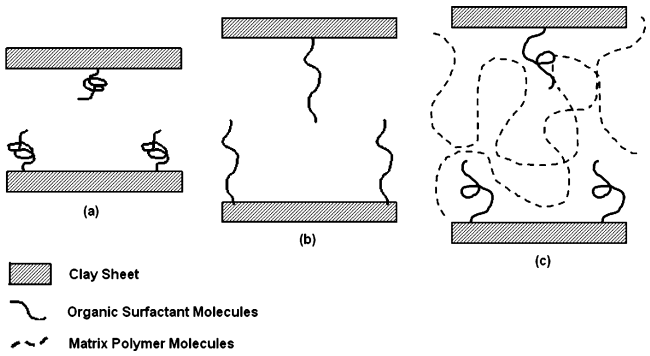

Figure 4. Disrupting effect of "very low coverage" on surfactant conformation: (a) "unperturbed" conformation; (b) "extended" conformation to fill space at very low coverage; (c) relief of nonequilibrium conformation by matrix polymer intercalation.

For example, at a surfactant coverage of ~17% (partial coverage), the actual area available per cation is about 1047 Å^2. Comparison of this area with the ideal required area per cation (πR_g^2) for each of the different surfactants shows that only surfactants Q-2 and Q-3 require less area per cation than is available. This indicates that there should be a difference in the conformation of the surfactant chains occupying the interlayer spaces in the clay, consequently presenting different environments to the intercalating matrix polymer when annealed to form the nanocomposite. A schematic representation of this idea is presented in Figure 4.

In the case of the modified clay M-2P, where the area available per cation (1047 Å^2) is in considerable excess of the area required by the unperturbed surfactant (380 Å^2) (Figure 4a), either the surfactant chains would be forced to stretch out to fill all available space in the galleries or the clay layers would have to deform greatly over a very short length scale. While clay layers are readily deformed on a 100 nm length scale, significant deformation at the 1 nm length scale is difficult because of the crystalline nature of the clay layers. A combination of these two possibilities is most probable. As a result, the surfactant chains are forced into an elongated, nonequilibrium conformation (Figure 4b), accompanied by some disruption in the ordered structure of the clay tactoids. Annealing in the presence of the matrix polymer may relieve this energetically unfavorable situation through intercalation of matrix polymer, further disrupting the regular stacking of the layered silicate tactoids (Figure 4c). For longer surfactants, the surfactant chains fill all available space in the galleries of the modified clay, preventing further entry of matrix homopolymer molecules.

This idea implies that nanocomposite morphology is a function of both surfactant length and the areal density of

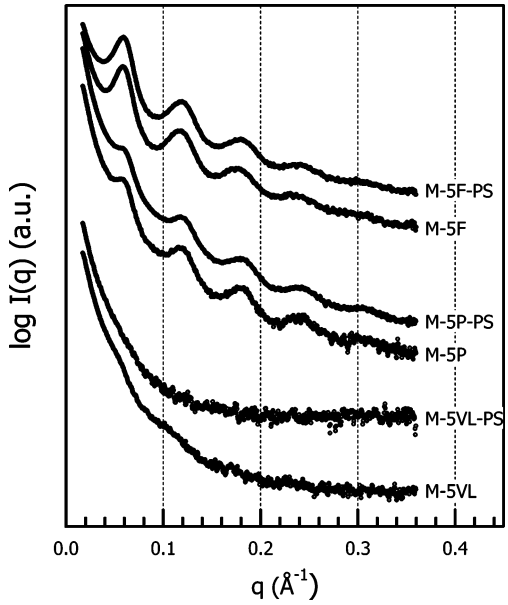

Figure 5. SAXS data contrasting the dramatic effect of "extent of silicate modification" on morphology of both modified clays and corresponding nanocomposites, for a series of PS-matrix-based PLSNs, using a surfactant of 5.5 kg/mol molecular weight.

surfactants on the silicate clay surface. For a given surfactant length, lowering coverage should eventually result in modified clay that can be disordered simply by annealing. Similarly, for a given coverage, there should be a critical surfactant length below which disruption of the clay tactoid would occur. This relationship between morphology, surfactant areal density, and surfactant length suggests that nanocomposite morphology could effectively be controlled by tailoring the coverage of the clay as a function of surfactant modifier molecular weight.

To test this idea, layered silicate was again modified with a longer surfactant, Q-5, that at 17% coverage had produced only phase-separated morphologies. However, in this experiment, the clay was modified to "very low" coverage in the hope of accessing the window of phase space described above, in which tailoring the surfactant areal density for a given surfactant length creates a kinetically trapped, nonequilibrium state that causes the clay tactoid to become disordered on annealing, as was seen in the case of M-2P-PS. From Table 3, for surfactant Q-5, of approximate molecular weight 5.5 kg/mol, R_g is calculated to be roughly 21 Å, which translates into an area ∼1386 Å^2 per Q-5 cation that would be required in order for it to adopt the ideal random coil configuration. Because the required area per cation (1386 Å^2) is greater than the available area per cation (1047 Å^2) in the modified clay, M-5P, the Q-5 surfactant molecules would fill all available gallery space and exclude any matrix molecule intercalation on annealing the modified clay in the presence of a homopolymer matrix. To recreate the kinetically trapped, nonequilibrium state postulated to occur in M-2P, using Q-5, a coverage of ∼5% of the total available CEC sites by the surfactant was required. This "very low" coverage would provide conditions where the available area per cation (3825 Å^2) was much greater than the required area for each molecule. This condition would be qualitatively similar to that for surfactant Q-2 at the partial (17%) coverage level, where the available area was ∼2.75 times the "required" area per cation. The resulting modified clay (M-5VL) was then used to make the corresponding PS matrix based-nanocomposite, M-5VL-PS. To complete the study of morphology as a function of surfactant coverage, clay was also modified as fully as possible (M-5F) and then direct melt annealed as before with PS-homopolymer (M-5F-PS). This provided a complete set of samples based on surfactant Q-5, with coverage varying from "full" to "partial" to "very low", which could be used to systematically examine the effect of coverage on morphology. These samples would allow testing of the hypothesis that as long as the area available to a surfactant molecule is well above the area required for the surfactant to adopt its ideal random coil conformation, the clay tactoids will disorder, thus providing a route to the subsequent formation of intercalated and exfoliated PLSNs.

The SAXS data for M-5VL and M-5VL-PS are presented in Figure 5, along with the SAXS data for M-5F and M-5F-PS. Figure 5 also gives the SAXS data for M-5P and M-5P-PS (drawn from Figure 1), for ease of comparison. Representative micrographs from the TEM data collected for the complete series of samples based on the Q-5 surfactant are presented in Figure 6.

No change in the SAXS data for the full coverage samples is noted, indicating that no intercalation or mixing of any kind occurred. This is consistent with the very large, well-ordered clay tactoid shown in Figure 6a. Figure 6b shows a smaller, but similarly well-ordered, clay tactoid observed in M-5P-PS, consistent with the SAXS data presented in Figure 1. However, weak Bragg reflections for M-5VL can be discerned in Figure 5 as well as an absence of any reflections from M-5VL-PS. These SAXS data are nearly identical to that of M-2P-PS. The major difference is only that the Bragg reflections for the modified clay, M-5VL, are so broad and weak that they are difficult to discern. This is most likely due to disorder of the second kind, where the distance between the clay sheets fluctuates about some average value, but no long-range periodicity is present. More telling is the micrograph shown in

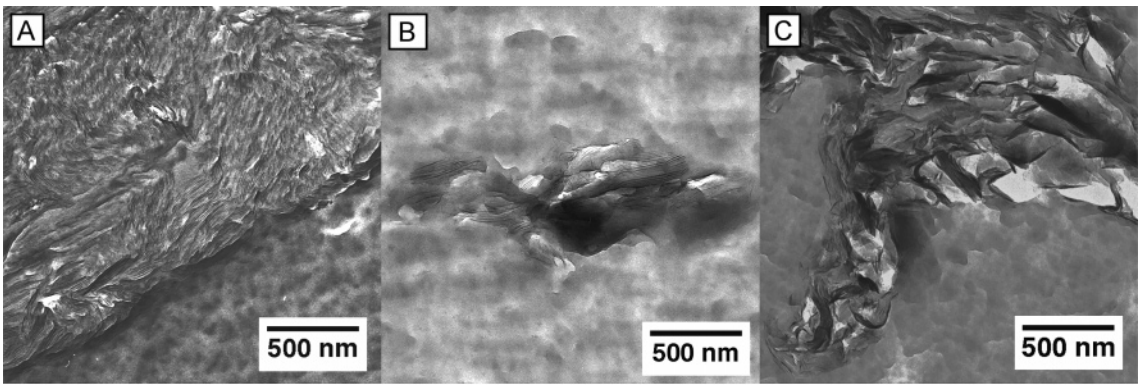

Figure 6. TEM micrographs showing (A) M-5F-PS, (B) M-5P-PS, and (C) M-5VL-PS. The image of M-5VL-PS clearly shows an unusual tactoid morphology, similar to crumpled paper, with no visible evidence of stacks of layers readily found in most PLSNs.

Figure 6c of a large tactoid found in sample M-5VL-PS. There is no region of ordered layers in the M-5VL-PS tactoid, unlike most tactoids that always show some region in which stacks of clay layers are visible, such as those shown in Figure 6a,b. In cases where mechanical techniques such as extrusion are employed to aid silicate dispersion in the polymer matrix, micrographs indicative of exfoliated morphologies generally show individual silicate layers and/or bundles of a few silicate layers, dispersed in the polymer matrix with a preferred direction of orientation imparted by the extruder.[50] In the present case, where no mechanical mixing was used, large tactoids were commonly observed, but no evidence of periodic stacks of sheets was seen. It must also be noted that, in the absence of mechanical mixing, most of the volume of the samples was unmodified matrix.

A final point to consider is that there must exist bounds on the range of surfactant lengths which will cause the clay tactoids to become disordered. If relief of a nonequilibrium, kinetically trapped state is the driving force for the disruption of the tactoid ordering, then only when the surfactant is long enough to create that state will this driving force exist, defining a lower bound. For example, modification of clay with a small "cation" such as ammonium does not automatically lead to disordering. On the other hand, intuitively, it is easy to appreciate that it would be increasingly difficult to get uniform coverage of a given amount of clay using a progressively smaller number of "long" cations, thus creating an upper bound. Relatively large surfactant molecules also present practical challenges in the clay modification process, since these organic surfactants are often insoluble in aqueous media and thus require aqueous/organic mixtures. Hence, a balance must be reached between surfactant length, effectively disordering the clay tactoids, and achieving good surfactant coverage.

Conclusions

Using a set of model, quaternary amine-terminated PS-based surfactants, the morphological behavior of a series of model polymer-layered silicate nanocomposites was examined. Montmorillonite clay was modified "partially" by exchanging the naturally occurring sodium cations with PS-based surfactants until ~17% of the available cations were exchanged. PLSNs made from these modified clays via direct melt intercalation of PS homopolymer ($\chi = 0$) generally showed phase-separated morphologies, consistent with previous studies using higher loadings of surfactant. Samples made from the same modified clays and matrices of PVME ($\chi < 0$) and PMMA ($\chi > 0$) showed that the enthalpic interactions between the polymer matrix and PS-based surfactant had only marginal effects on morphological behavior.

However, it was also observed that PLSNs made from clays that were modified such that the area available on the silicate surface per surfactant cation was at least 3 times the actual area required by the cation to adopt an equilibrium conformation, such as in the case of M-2P-PS, lost essentially all evidence of ordered clay stacks upon annealing. This is thought to be due to the creation of a kinetically trapped, nonequilibrium state within the modified clay, where the surfactant molecules are at such a low areal density that they adopt highly distorted, nonequilibrium conformations to fill the available gallery space. Annealing these modified clays in the presence of homopolymer relieves this unstable state, allowing the clay tactoids to become more disordered, most likely through the intercalation of matrix polymer.

In a second set of experiments, a longer surfactant, Q-5, was used to create modified clay with surfactant coverage of 4.7%, providing each cation with ~3 times the area it required on the surface. This condition was chosen to be identical to that for Q-2 at 17% coverage. The same disordering behavior was observed, where TEM data revealed that that clay layers were not dispersed as in the traditional sense of an exfoliated morphology despite the featureless SAXS data, but rather remained in tactoid-like clumps without any ordered stacking of the layers.

These results validate the idea that coverage and surfactant length, the two critical factors that determine nanocomposite morphology, can be adjusted to induce clay tactoid disruption. Though the two factors are related and it is difficult to conclusively elucidate whether one is more important than the other for promoting intercalation, the current investigation demonstrates an empirical method for determining the coverage that will promote intercalation for a given surfactant length. Additionally, this effect is more important than the enthalpic interaction between the surfactant and polymer. This may be a technologically important development; an energetically favorable route to disruption of clay tactoids should simplify the processing requirements for fabricating exfoliated PLSNs. Less energy intensive and damaging mixing processes would be required to create exfoliated PLSNs. The relative insensitivity of this process to the miscibility of matrix polymer and surfactant modifier also potentially opens this dispersion process to many combinations of matrix polymer and surfactant, hopefully enabling the more widespread application of PLSN materials.

Acknowledgment. The authors acknowledge financial support from the Army Research Laboratory Materials Center of Excellence in Composite Materials, Contract DAAD19-01-2-001, located at the Center for Composite Materials, University of Delaware, Newark, DE. Mr. Ziegler was supported through a Research Participation Program Fellowship administered by the Oak Ridge Institute for Science and Education.

References and Notes

(1) Yano, K.; Usuki, A.; Okada, A.; Kurauchi, T.; Kamigaito, O. *J. Polym. Sci., Part A: Polym. Chem.* **1993**, *31*, 2493−2498.
(2) Chen, C.; Tolle, T. B. *J. Polym. Sci., Part B: Polym. Phys.* **2004**, *42*, 3981−3986.
(3) Shen, Z.; Simon, G. P.; Cheng, Y.-B. *J. Appl. Polym. Sci.* **2004**, *92*, 2101−2115.
(4) Ahmadi, S. J.; Huang, Y. D.; Li, W. *J. Mater. Sci.* **2004**, *39*, 1919−1925.
(5) Li, X. C.; Ha, C. S. *J. Appl. Polym. Sci.* **2003**, *87*, 1901−1909.
(6) McNally, T.; Raymond Murphy, W.; Lew, C. Y.; Turner, R. J.; Brennan, G. P. *Polymer* **2003**, *44*, 2761−2772.
(7) Chang, J. H.; An, Y. U.; Cho, D. H.; Giannelis, E. P. *Polymer* **2003**, *44*, 3715−3720.
(8) Lepoittevin, B.; Pantoustier, N.; Devalckenaere, M.; Alexandre, M.; Calberg, C.; Jerome, R.; Henrist, C.; Rulmont, A.; Dubois, P. *Polymer* **2003**, *44*, 2033−2040.
(9) Zanetti, M.; Kashiwagi, T.; Falqui, L.; Camino, G. *Chem. Mater.* **2002**, *14*, 881−887.
(10) Krikorian, V.; Kurian, M.; Galvin, M. E.; Nowak, A. P.; Deming, T. J.; Pochan, D. J. *J. Polym. Sci., Part B: Polym. Phys.* **2002**, *40*, 2579−2586.
(11) Shen, Z. Q.; Simon, G. P.; Cheng, Y. B. *Polymer* **2002**, *43*, 4251−4260.
(12) Alexandre, M.; Dubois, P.; Sun, T.; Garces, J. M.; Jerome, R. *Polymer* **2002**, *43*, 2123−2132.
(13) Dennis, H. R.; Hunter, D. L.; Chang, D.; Kim, S.; White, J. L.; Cho, J. W.; Paul, D. R. *Polymer* **2001**, *42*, 9513−9522.
(14) Lincoln, D. M.; Vaia, R. A.; Wang, Z. G.; Hsiao, B. S. *Polymer* **2001**, *42*, 1621−1631.
(15) Huang, X. Y.; Brittain, W. J. *Macromolecules* **2001**, *34*, 3255−3260.
(16) LeBaron, P. C.; Wang, Z.; Pinnavaia, T. J. *Appl. Clay Sci.* **1999**, *15*, 11−29.
(17) Bergman, J. S.; Chen, H.; Giannelis, E. P.; Thomas, M. G.; Coates, G. W. *Chem. Commun.* **1999**, *21*, 2179−2180.

(18) Weimer, M. W.; Chen, H.; Giannelis, E. P.; Sogah, D. Y. *J. Am. Chem. Soc.* **1999**, *121*, 1615−1616.
(19) Messersmith, P. B.; Giannelis, E. P. *Chem. Mater.* **1993**, *5*, 1064−1066.
(20) Aranda, P.; Ruizhitzky, E. *Chem. Mater.* **1992**, *4*, 1395−1403.
(21) Vaia, R. A.; Vasudevan, S.; Krawiec, W.; Scanlon, L. G.; Giannelis, E. P. *Adv. Mater.* **1995**, *7*, 154−156.
(22) Liao, B.; Song, M.; Liang, H. J.; Pang, Y. X. *Polymer* **2001**, *42*, 10007−10011.
(23) Vaia, R. A.; Sauer, B. B.; Tse, O. K.; Giannelis, E. P. *J. Polym. Sci., Part B: Polym. Phys.* **1997**, *35*, 59−67.
(24) Kawasumi, M.; Hasegawa, N.; Kato, M.; Usuki, A.; Okada, A. *Macromolecules* **1997**, *30*, 6333−6338.
(25) Kato, M.; Usuki, A.; Okada, A. *J. Appl. Polym. Sci.* **1997**, *66*, 1781−1785.
(26) Solomon, M. J.; Almusallam, A. S.; Seefeldt, K. F.; Somwangthanaroj, A.; Varadan, P. *Macromolecules* **2001**, *34*, 1864−1872.
(27) Lan, T.; Pinnavaia, T. J. *Chem. Mater.* **1994**, *6*, 2216−2219.
(28) Messersmith, P. B.; Giannelis, E. P. *Chem. Mater.* **1994**, *6*, 1719−1725.
(29) Vaia, R. A.; Jandt, K. D.; Kramer, E. J.; Giannelis, E. P. *Macromolecules* **1995**, *28*, 8080−8085.
(30) Vaia, R. A.; Jandt, K. D.; Kramer, E. J.; Giannelis, E. P. *Chem. Mater.* **1996**, *8*, 2628−2635.
(31) Vaia, R. A.; Giannelis, E. P. *Macromolecules* **1997**, *30*, 7990−7999.
(32) Vaia, R. A.; Giannelis, E. P. *Macromolecules* **1997**, *30*, 8000−8009.
(33) Ren, J. X.; Silva, A. S.; Krishnamoorti, R. *Macromolecules* **2000**, *33*, 3739−3746.
(34) Jang, B. N.; Wang, D.; Wilkie, C. A. *Macromolecules* **2005**, *38*, 6533−6543.
(35) Manias, E.; Touny, A.; Wu, L.; Strawhecker, K.; Lu, B.; Chung, T. C. *Chem. Mater.* **2001**, *13*, 3516−3523.
(36) Lyatskaya, Y.; Balazs, A. C. *Macromolecules* **1998**, *31*, 6676−6680.
(37) Balazs, A. C.; Singh, C.; Zhulina, E. *Macromolecules* **1998**, *31*, 8370−8381.
(38) Aranda, P.; Ruiz-Hitzky, E. *Chem. Mater.* **1992**, *4*, 1395−1403.
(39) Aranda, P.; Ruiz-Hitzky, E. *Appl. Clay Sci.* **1999**, *15*, 119−135.
(40) Beyer, F. L.; Tan, N. C. B.; Dasgupta, A.; Galvin, M. E. *Chem. Mater.* **2002**, *14*, 2983−2988.
(41) Kurian, M.; Dasgupta, A.; Beyer, F. L.; Galvin, M. E. *J. Polym. Sci., Part B: Polym. Phys.* **2004**, *42*, 4075−4083.
(42) Burnside, S. D.; Wang, H. C.; Giannelis, E. P. *Chem. Mater.* **1999**, *11*, 1055−1060.
(43) Long, D.; Ajdari, A.; Leibler, L. *Langmuir* **1996**, *12*, 1675−1680.
(44) Rhoades, J. D. *Cation Exchange Capacity*; American Society of Agron., Inc.: Madison, WI, 1982.
(45) Ross, D. S. *Recommended Methods for Determining Soil Cation Exchange Capacity*; Northeastern Regional Publication No. 493 Revised; University of Delaware Expt. Stat.: Newark, DE, 1995.
(46) Van Olphen, H. *An Introduction to Clay Colloid Chemistry*; Interscience Publishers: New York, 1963.
(47) Balsara, N. P. In *Physical Properties of Polymers Handbook*; Mark, J. E., Ed.; AIP Press: New York, 1996; pp 257−268.
(48) Roe, R.-J. *Methods of X-ray and Neutron Scattering in Polymer Science*; Oxford University Press: New York, 2000.
(49) Vaia, R. A.; Liu, W. D. *J. Polym. Sci., Part B: Polym. Phys.* **2002**, *40*, 1590−1600.
(50) Choi, Y. S.; Chung, I. J. *Polymer* **2004**, *45*, 3827−3834.

MA052478Z